found to cause a partial change in the monolayer morphology resulting in some blocked channels that were not completely filled. Unfilled channels (shown as dark in Fig. 3) can be clearly distinguished from filled ones in the SFM phase image due to the difference in their viscoelasticity[30]. This material contrast has been pursued over macroscopic distances moving along the 'attolitre' liquid cavities formed by the channels (a single channel that is 1 cm in length can hold up to four attolitres).

Third, a small droplet of $FeCl_3$ solution was brought onto the structured mica surface and evaporated slowly. The $FeCl_3$ molecules condensing from the vapour phase were selectively adsorbed in the guiding channels, whereas the monolayer stripes were not coated (Fig. 4, top). The SFM images were taken at positions several centimetres away from the droplet. Channels filled with $FeCl_3$ molecules provide a contrast in magnetic force microscopy as shown in Fig. 4, bottom.

This method should not be restricted to a specific adsorbate-and-substrate pair and may be extended to other rapidly adsorbing amphiphilic molecules and polymers; however, no other distinct adsorbate-and-substrate pair has yet been investigated. The tiniest channels obtained so far with this method are about 100 nm in width corresponding to a channel density of 20,000 cm^{-1}. Such nano-channel arrays over macroscopic areas may find potential applications as chemical or biochemical reaction cavities with attolitre capacity, in analytical separation techniques, and as textured surfaces.

1. Barthlott, W. & Neinhuis, C. Purity of the sacred lotus, or escape from contaminations in biological surfaces. *Planta* **202**, 1–8 (1997).
2. Wagner, T., Neinhuis, C. & Barthlott, W. Wettability and contaminability of insect wings as a function of their surface sculpture. *Acta Zool.* **77**, 213–225 (1996).
3. Böltau, M., Walheim, S., Mlynek, J., Krausch, G. & Steiner, U. Surface-induced structure formation of polymer blends on patterned surfaces. *Nature* **391**, 877–879 (1998).
4. Gallardo, B. S. *et al.* Electrochemical principles for active control of liquids on submillimeter scales. *Nature* **283**, 57–60 (1999).
5. Delamarche, E., Bernard, A., Schmid, H., Michel, B. & Biebuyck, H. Patterned delivery of immunoglobulins to surfaces using microfluidic networks. *Science* **276**, 779–781 (1997).
6. Harrison, D. J. *et al.* Micromachining a miniaturized capillary electrophoresis-based chemical analysis system on a chip. *Science* **261**, 895–897 (1993).
7. Kumar, A., Biebuyk, H. A. & Whitesides, G. M. Patterning self-assembled monolayers: applications in materials science. *Langmuir* **10**, 1498–1511 (1994).
8. Xia, Y. & Whitesides, G. M. Extending microcontact printing as a microlithographic technique. *Langmuir* **13**, 2059–2067 (1997).
9. Evans, S. D., Flynn, T. M. & Ulman, A. Self-assembled multilayer formation on predefined templates. *Langmuir* **11**, 3811–3814 (1995).
10. Abott, N. L., Folkers, J. P., Whitesides, G. M. Manipulation of the wettability of surfaces on the 0.1–1-micrometer scale through micromachining and molecular self-assembly. *Science* **257**, 1380–1382 (1992).
11. Wang, R. *et al.* Light induced amphiphilic surfaces. *Nature* **388**, 431–432 (1997).
12. Calvert, J. M. Lithographic patterning of self-assembled films. *J. Vac. Sci. Technol. B* **11**(6), 2155–2163 (1993).
13. Gau, H., Herminghaus, S., Lenz, P. & Lipowsky, R. Liquid morphologies on structured surfaces: from microchannels to microchips. *Science* **283**, 46–49 (1999).
14. Wittmann, J. C. & Smith, P. Highly oriented thin films of poly(tetrafluoroethylene) as a substrate for oriented growth of materials. *Nature* **352**, 414–417 (1991).
15. Kuhn, H., Möbius, D. & Bücher, H. in *Physical Methods of Chemistry*, Vol. 1 (3b) (eds Weisenberger, A. & Rossiter, B.) 577–702 (Wiley, New York, 1972).
16. Petrov, J. G., Kuhn, H. & Möbius, D. Three-phase contact line motion in the deposition of spread monolayers. *J. Colloid Interface Sci.* **37**, 66–75 (1980).
17. Riegler, H. & Spratte, K. Structural changes in lipid monolayers during the Langmuir-Blodgett transfer due to substrate / monolayer interactions. *Thin Solid Films* **210/211**, 9–12 (1992).
18. Neumann, A. W. Contact angles and their temperature dependence: thermodynamic status, measurement, interpretation and application. *Adv. Colloid Interface Sci.* **59**, 105–191 (1972).
19. Spratte, K., Chi, L. F. & Riegler, H. Physisorption instabilities during dynamic Langmuir wetting. *Europhys. Lett.* **25**, 211–217 (1994).
20. Erikson, L. G. T., Cleasson, P. M., Ohnishi, S. & Hato, M. Stability of dimethyldioctadecylammonium bromide Langmuir-Blodgett films on mica in aqueous salt solutions—implications for surface force measurements. *Thin Solid Films* **300**, 240–255 (1997).
21. Langer, J. S. Issues and opportunities in materials research. *Phys. Today* 24–31 (1992).
22. Zasadzinski, J. A. N. & Schneider, M. B. Ripple wavelength, amplitude, and configuration in lyotropic liquid crystals as a function of effective headgroup size. *J. Phys. (France)* **48**, 2001–2011 (1987).
23. Maske, H. A., Havlin, S., King, P. R. & Stanley, E. Spontaneous stratification in granular mixtures. *Nature* **386**, 379–382 (1997).
24. Bowden, N., Brittain, S., Evans, A. G., Hutchinson, J. W. & Whitesides, G. M. Spontaneous formation of ordered structures in thin films of metals supported on an elastomeric polymer. *Nature* **393**, 146–149 (1998).
25. Weis, R. M. & McConnell, H. M. Cholesterol stabilizes the crystal-liquid interface in phospholipid monolayers. *J. Phys. Chem.* **89**, 4453–4459 (1985).
26. Chunbo, Y. *et al.* Lanthanide ion induced formation of stripes domain structure in phospholipid Langmuir-Blodgett monolayers film observed by atomic force microscopy. *Surf. Sci.* **366**, L729–L734 (1996).
27. Biebuyck, H. A. & Whitesides, G. M. Self-organisation of organic liquids on patterned self-assembled monolayers of alkanthiols on gold. *Langmuir* **10**, 2790–2793 (1994).
28. Kim, E., Xia, Y. & Whitesides, G. M. Polymer microstructures formed by moulding in capillaries. *Nature* **376**, 581–584 (1995).
29. Xia, Y. & Whitesides, G. M. Soft Lithography. *Annu. Rev. Mater. Sci.* **28**, 153–184 (1998).
30. Anczykowski, B., Gotsmann, B., Fuchs, H., Cleveland, J. P. & Elings, V. B. How to measure energy dissipation in dynamic mode atomic force microscopy. *Appl. Surf. Sci.* **140**, 376–382 (1999).

DNA computing on surfaces

Qinghua Liu*†, Liman Wang*, Anthony G. Frutos*†, Anne E. Condon†‡, Robert M. Corn* & Lloyd M. Smith*

* Department of Chemistry, ‡ Department of Computer Science, University of Wisconsin, Madison, Wisconsin 53706, USA

DNA computing was proposed[1] as a means of solving a class of intractable computational problems in which the computing time can grow exponentially with problem size (the 'NP-complete' or non-deterministic polynomial time complete problems). The principle of the technique has been demonstrated experimentally for a simple example of the hamiltonian path problem[2] (in this case, finding an airline flight path between several cities, such that each city is visited only once[3]). DNA computational approaches to the solution of other problems have also been investigated[4–9]. One technique[10–13] involves the immobilization and manipulation of combinatorial mixtures of DNA on a support. A set of DNA molecules encoding all candidate solutions to the computational problem of interest is synthesized and attached to the surface. Successive cycles of hybridization operations and exonuclease digestion are used to identify and eliminate those members of the set that are not solutions. Upon completion of all the multi-step cycles, the solution to the computational problem is identi-fied using a polymerase chain reaction to amplify the remaining molecules, which are then hybridized to an addressed array. The advantages of this approach are its scalability and potential to be automated (the use of solid-phase formats simplifies the complex repetitive chemical processes, as has been demonstrated in DNA and protein synthesis[14]). Here we report the use of this method to solve a NP-complete problem. We consider a small example of the satisfiability problem (SAT)[2], in which the values of a set of boolean variables satisfying certain logical constraints are deter-mined.

Our overall strategy for DNA computing on surfaces has been described in detail previously[10], and consists of six main steps shown diagrammatically in Fig. 1. Each step in the process must be reasonably efficient for the overall process to succeed; the development of these steps has been the subject of previous work[10–12], and may be briefly summarized as follows. Oligonucleotides are synthesized individually, and pooled or arrayed on surfaces as needed. The 5′ thiol-modified oligonucleotides (S_xs) are attached to the surface in an unaddressed fashion; compared to addressed oligonucleotide

† Present addresses: Gen-Probe, Inc., San Diego, California 92121, USA (Q.L.); Corning Inc., Corning, New York 14831, USA (A.G.F.); Department of Computer Science, University of British Columbia, Vancouver, BC V6T 1Z4, Canada (A.E.C.).

arrays[15,16], this allows a greater number of different sequences to be deposited per unit area, but necessitates the use of a final 'readout' step to determine the identity of the remaining oligonucleotides once the computation has been performed[10]. Each DNA "word"[11] consists of 16 nucleotides with the structure 5′-FFFFvvvvvvvvFFFF-3′; the internal eight nucleotides ('v')are variables and encode the information (Table 1); the eight bases labelled 'F' are fixed 'word labels' that direct DNA hybridization of 16 nucleotide complements to that word in the 'mark' operation. The prototype DNA computer described here uses a single word. SAT computation is done through repeated cycles of 'mark', 'destroy' and 'unmark' operations[10] (Fig. 1). Finally, determination of the 'answer' to the computational problem of interest is accomplished in a 'readout' operation (see Methods). We note that other investigators have also reported surface-based approaches to DNA computing; indeed, Adleman's first report of DNA computing utilized support chemistry to separate DNA molecules[1]; and more recently, Morimoto *et al.*[17] and Yoshida and Suyama[18] have described solid-phase procedures for DNA computing.

The SAT problem is an NP-complete problem in boolean logic[2]. An instance of the SAT problem consists of a set of boolean logic variables separated by the logical OR operation (denoted by "$\vee$"; $u \vee v = 0$ if and only if $u = v = 0$) within clauses, and with the clauses separated by the logical AND operation (denoted by "$\wedge$"; $u \wedge v = 1$ if and only if $u = v = 1$). The problem is to find whether there are values for the variables that simultaneously satisfy each clause in a given instance of the problem[2]. The specific SAT problem solved here is:

$$(w \vee x \vee y) \wedge (w \vee \bar{y} \vee z) \wedge (\bar{x} \vee y) \wedge (\bar{w} \vee \bar{y})$$

and employs four variables w, x, y and z ($\bar{w}$, $\bar{x}$, $\bar{y}$ and $\bar{z}$ denote the negation of the variables w, x, y and z; thus $\bar{w} = 0$ if and only if $w = 1$,

and $\bar{w} = 1$ if and only if $w = 0$). Each of the four variables can be either true (1) or false (0) and thus there are total of 2^4 or 16 candidate solutions. All methods for solving the SAT problem (on any realizable computing device) that have been analysed require a number of steps that grows exponentially with the number of variables. However, algorithms have been developed for conventional computing which substantially decrease the difficulty of the problem compared to a 'brute-force' search through all possible solutions. For example, the best known algorithm for the 3-SAT problem, in which the number of variables per clause is at most 3, has expected running time bounded by a polynomial time 1.33^n for large n (ref. 19), a very substantial improvement compared to the 2^n running time characteristic of the 'brute-force' search. It has recently been shown that such algorithms may also be implemented in DNA computing approaches, including specifically the 3-SAT problem addressed here[6,18]. We show here how 3-SAT may be solved using immobilized DNA molecules and a simple 'brute-force' search strategy; the more complex operations required to execute more sophisticated algorithms are under development.

The surface-bound oligonucleotide sequences utilized were of the form 5′-HS-C_6-T_{15}GCTTvvvvvvvvTTCG-3′ (S_xs). The T_{15} sequence serves as a 'spacer' group to separate the hybridizing sequence from the support[20], the GCTT and TTCG sequences are the 'word label' used to target hybridization to a particular word[11], and the v_8 sequence is used to encode information. Table 1 shows the 16 octanucleotide sequences used, which were chosen from a previously described set of 108 possible sequences[11], along with the encoding scheme utilized to represent the possible values of the SAT variables w, x, y and z. These surface-bound oligonucleotides, representing all candidate solutions, were synthesized, pooled, and attached to a maleimide-functionalized gold surface in an unaddressed format[21,22]. Each clause of the SAT problem requires one cycle of 'mark', 'destroy' and 'unmark' (Fig. 1), and thus four cycles were employed to solve the example SAT problem above. The goal of the first computational cycle is to destroy all DNA molecules which do not satisfy the first clause ($w \vee x \vee y$). This is achieved by hybridizing to the surface those oligonucleotides that are complementary to the molecules which do satisfy the clause, and then destroying the remaining (unmarked) single-stranded molecules. Only two sequences do not satisfy this clause: namely, those for which w, x and y are set to zero (S_0 [0000] and S_1 [0001], see Table 1). Thus in cycle 1 the complements (C_xs) of the 14 other oligonucleotides ($w = 1$ (C_8, C_9, C_{10}, C_{11}, C_{12}, C_{13}, C_{14}, C_{15}); $x = 1$ (C_4, C_5, C_6, C_7, C_{12}, C_{13}, C_{14}, C_{15}); $y = 1$ (C_2, C_3, C_6, C_7, C_{10}, C_{11}, C_{14}, C_{15})) were combined and hybridized (in the 'mark' operation) to the surface; after washing, the surface was exposed to *Escherichia coli* exonuclease I to destroy the unhybridized, single-stranded molecules S_0 and S_1 (in the 'destroy' operation). The surface was regenerated
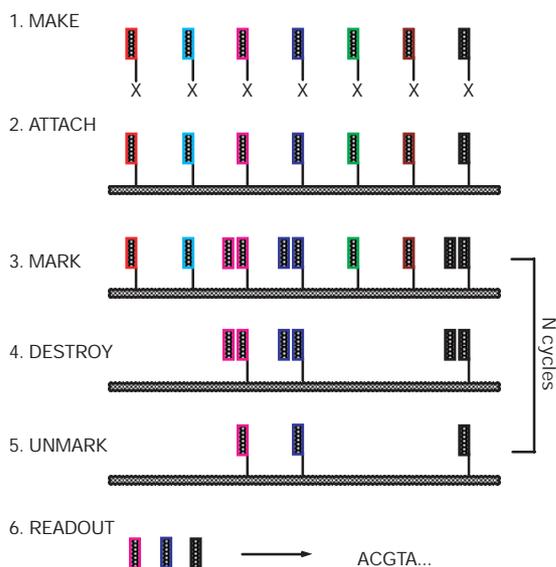

Figure 1 Overview of the surface-based approach to DNA computations. A combinatorial set of single-stranded DNA molecules representing all possible solutions to a given computational problem is synthesized ('make') and immobilized ('attach') on a surface via a reactive functional group X. In each of *N* successive cycles of the DNA computation, subsets of the surface-bound combinatorial mixture are tagged by hybridization to their complements in a 'mark' operation, rendering them double-stranded. After the 'mark' operation, an enzyme (for example, *Escherichia coli* exonuclease I) is added which destroys surface-bound oligonucleotides present in an unhybridized single-stranded form ('destroy'). The surface is then regenerated by removing all hybridized complements in an 'unmark' operation. Repetitive cycles of 'mark', 'destroy' and 'unmark' operations remove from the surface all strands which do not satisfy the problem. At the end of *N* cycles, only those strands which are solutions to the problem remain. Their identities are determined in a 'readout' operation by PCR followed by hybridization to an addressed array.

Table 1 Variable sequences and encoding scheme

Strand	Variable sequence	*wxyz*
S_0	CAACCCAA	0000
S_1	TCTCAGAG	0001
S_2	GAAGGCAT	0010
S_3	AGGAATGC	0011
S_4	ATCGAGCT	0100
S_5	TTGGACCA	0101
S_6	ACCATTGG	0110
S_7	GTTGGGTT	0111
S_8	CCAAGTTG	1000
S_9	CAGTTGAC	1001
S_{10}	TGGTTTGG	1010
S_{11}	GATCCGAT	1011
S_{12}	ATATCGCG	1100
S_{13}	GGTTCAAC	1101
S_{14}	AACCTGGT	1110
S_{15}	ACTGGTCA	1111

The 16 strands shown encode 4 bits (2^4) of information (4 variables: w, x, y, z). S_x is the 16-nucleotide DNA sequence 5′-GCTTv$_8$TTCG-3′, where the v_8 sequence is shown as the ''Variable sequence'' above; C_x is the 16-nucleotide complement of the S_x sequence.

by the 'unmark' operation to return the remaining surface-bound oligonucleotides S_2–S_{15} to single-stranded form. This process was repeated three more times for the remaining three clauses, to yield a surface containing only the solutions to the SAT problem.

In Fig. 2 we show in detail the logic of the DNA computation in each cycle, leading at the end to four types of DNA molecules remaining on the surface. It may be noted that since each clause is tested independently, in some cases complements are added corresponding to surface-bound oligonucleotides that are no longer on the surface, having been destroyed in a previous cycle. Although this entails some redundancy, the independence of clause-testing obtained in this manner increases the computational versatility and power. In the particular SAT problem solved here, each strand is destroyed only once (that is, is targeted in only one of the four computational cycles). The identity of those molecules that correspond to the solutions was determined at the end of the computation by polymerase chain reaction (PCR) amplification and hybridization to an addressed array. The results are shown in Fig. 3, presented both as a fluorescence image and in histogram form.

The four spots with high fluorescence intensity in Fig. 3 correspond to the four expected solutions to the computational problem posed. The DNA sequences identified in the 'readout' step via addressed array hybridization were: S_3, S_7, S_8 and S_9 (Fig. 3). Their variable sequences are AGGAATGC, GTTGGGTT, CCAAGTTG,

and CAGTTGAC (Table 1), corresponding to the truth assignments of ($w = 0$, $x = 0$, $y = 1$, and $z = 1$), ($w = 0$, $x = 1$, $y = 1$, and $z = 1$), ($w = 1$, $x = 0$, $y = 0$, and $z = 0$), and ($w = 1$, $x = 0$, $y = 0$, and $z = 1$). For example, the assignment ($w = 0$, $x = 0$, $y = 1$, and $z = 1$) satisfies the SAT problem solved here in that $y = 1$ satisfies the first clause ($w \vee x \vee y$), $z = 1$ satisfies the second clause ($w \vee \bar{y} \vee z$), either $x = 0$ or $y = 1$ makes the third clause ($\bar{x} \vee y$) true, and $w = 0$ satisfies the last clause ($\bar{w} \vee \bar{y}$). The signal intensities for the spots corresponding to the correct solutions were 10 to 777 times greater than those corresponding to incorrect solutions, making discrimination between correct and incorrect solutions to the problem straightforward. We now consider the issues which need to be addressed for scaling of the approach to substantially larger problems.

Each step in the above-described DNA computing process is chemically complex and subject to error. For example, in the 'mark' operation, the nature of chemical reaction kinetics ensures that the hybridization-driven formation of duplex structures on the surface will be incomplete, and hence some surface-immobilized DNA molecules encoding correct answers to the clause in question will not form duplexes; these molecules will then be subject to unwanted destruction during the 'destroy' (exonuclease digestion) step, degrading signal during the computational process. Conversely, mismatch hybridization to incorrect sequences present on the surface may protect them inappropriately from destruction, leading to background signal corresponding to incorrect solutions to the problem.

In addition, the destruction of single-stranded DNA molecules on the surface by *E. coli* exonuclease I is not perfect. Approximately 94% of unmarked single-stranded immobilized DNA molecules can be removed by the exonuclease digestion reaction[11]. This means that about 6% of the unwanted (incorrect) DNA molecules will remain on the surface after a 'destroy' operation, giving rise to false positive
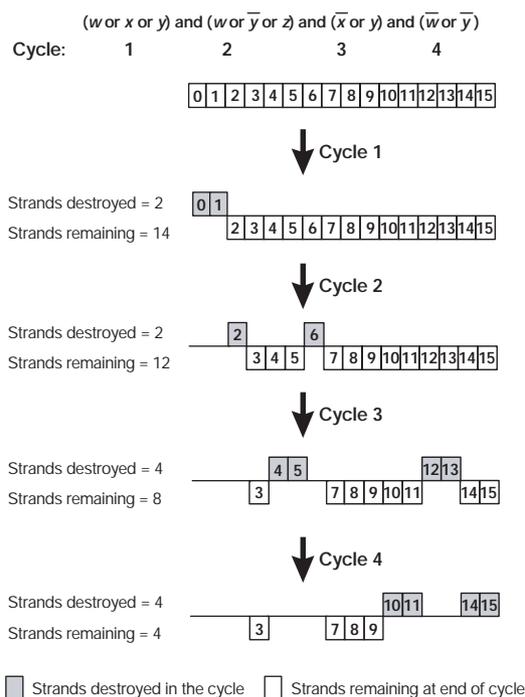

Figure 2 Four cycles of SAT computation. For each cycle of the computation, the number of strands destroyed in that cycle of the computation and the number of strands remaining on the surface at the end of the cycle are indicated on the left. The identities of the destroyed and remaining strands are shown in the progression of the computation in schematic form: in each cycle of computation one of the four clauses is tested by applying the 'mark' operation to only the oligonucleotides that satisfy that clause. For example, in cycle 1, applying the 'mark' operation to S_2 – S_{15} (leaving S_0 and S_1 unmarked) protects all the surface-bound oligonucleotides for which w or x or y has a value of 1. A similar procedure is applied in each of the three subsequent cycles for clauses 2 – 4, respectively. In each cycle, strands indicated in the shaded boxes are destroyed using the single-strand specific *E. coli* exonuclease I, while strands indicated in the non-shaded boxes are protected by their complements. The strands remaining in the non-shaded boxes at the end of the process are the solutions to the computational problem.
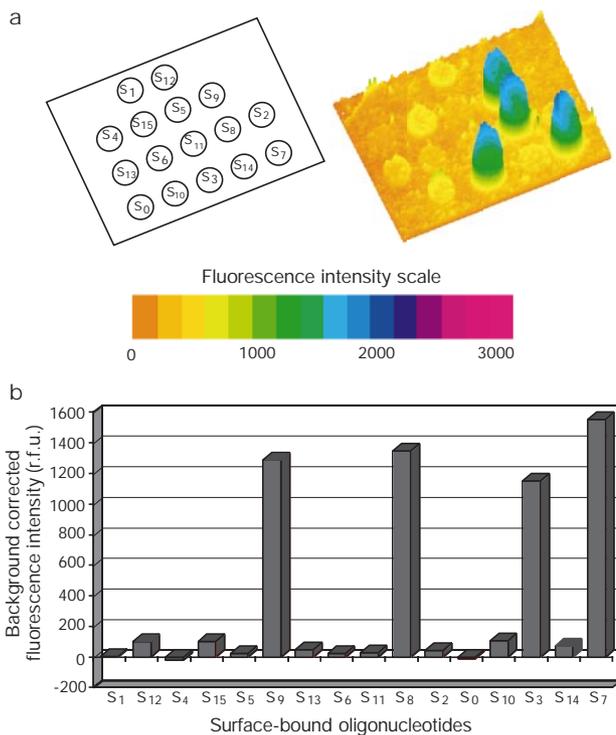

Figure 3 Three-dimensional plot and histogram of the fluorescence intensities on a 16 element addressed array used for 'readout'. **a,** Fluorescence profile (right) with the surface-bound oligonucleotide locations (left). **b,** The fluorescence intensity histogram. The three-dimensional plot in **a** was generated using NIH Image version 1.61 software (National Institutes of Health, Bethesda, Maryland; http://rsb.info.nih.gov/nih-image/download.html). r.f.u., relative fluorescence units.

signals. A more fundamental issue with the 'destroy' operation presented here is that it is incompatible with a multiple-word encoding strategy; work is in progress to develop an alternative 'destroy' operation for this purpose.

These errors in the 'mark' and 'destroy' operations also affect the 'readout' process. We have found it to be very difficult to uniformly amplify a population of DNA molecules, even ones as tightly constrained as the set employed here for DNA computing[23](data not shown). Small amounts of unwanted oligonucleotides, if amplified preferentially compared to desired species present initially at higher concentration, can yield aberrant results. Although the GC content was held constant for the set of DNA molecules used in this work, variations in the position of GC pairs within the sequence can affect the formation of secondary structures that influence the efficiency of PCR amplification. Betaine is known to preferentially destabilize GC base pairs[24]. The use of betaine here resulted in a more uniform amplification of the mixture of DNA templates[25]. Nonetheless, substantial optimization and experimentation with the PCR conditions were required to obtain the results shown here, and it is likely that this would become increasingly difficult with larger problems. This is fundamentally a reflection of the intrinsically nonlinear nature of the PCR amplification process[26]; an alternative method of amplification which is linear in nature is under investigation[27].

This intrinsically error-prone nature of the DNA computing process, however, does not rule out its operational practicality. The fundamental operations of conventional computing are also prone to error at the device level, and there is a rich body of knowledge on algorithmic solutions to these issues which could be adapted to the DNA computing process[28]. Methods for handling errors in DNA computations have been reported[29,30]. Experimental determination of error rates in surface-based DNA computing could provide the information necessary to develop error models and algorithmic methods to control errors in computations.

The surface approach described here was designed to permit scale-up to larger problems. For example, the use of six tandem words on the surface (for a total oligomer length of $16 \times 6 = 96$ nucleotides, within the range of current oligonucleotide synthesis capabilities), and 64 different octanucleotide sequences[11] to encode information in each of the words (6 bits per word), corresponds to a search space containing approximately 6.9×10^{10} candidate solutions (2^{36}; that is, a 36-bit DNA computer).

The number of 'mark' and 'destroy' operations required to solve the problem grows polynomially with the number of variables[13], in contrast to the search space which grows exponentially. Thus a 36-bit DNA computer would not look a great deal different from the 4-bit computer described here. The biggest practical issue (apart from those mentioned above) is the synthesis and handling of large numbers of oligonucleotides (1,536 oligonucleotides would be needed to carry out the 'mark' and readout' operations for a 6-word, 6 bits per word, DNA computer of this type; see Methods). Instrumentation to synthesize and handle such large numbers of oligonucleotides is available (ABI 3948 Nucleic Acid Synthesis and Purification System (Perkin Elmer); also see refs 15 and 16). Specialized problems might require far fewer oligonucleotides than this (see Methods).

Methods

PCR amplification for 'readout'.

56-mer PCR templates were synthesized with the following structure:

5′-tatttttgagcagtggctccCGAAvvvvvvvvAAGCtagctatctacaagattcag-3′
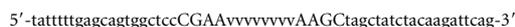
where the lower-case sequences are the two primers, the upper-case sequences are fixed word labels, and the eight bases labelled 'v' are complements of the variable regions shown in Table 1.

For PCR amplification and addressed array hybridization 'readout', the template(s) used in PCR amplification were collected from the computation chip (that is, the non-

addressed array surface which had undergone repetitive computation operations) as follows: upon completion of each computation cycle (including 'mark', 'destroy', 'unmark'), the coverslip (computation chip) was exposed to a mixture of all 16 complementary DNA strands (each containing two 20-mer primer sequences as indicated above) for 1.5 h for hybridization. The coverslip was then washed; all hybridized complements were melted off and collected by assembling the coverslip in a GeneAmp *In Situ* PCR System 1000 (Perkin Elmer) containing 100 µl of de-ionized water, and heating at 95 °C for 10 min. The collected template(s) were then amplified using biotinylated and fluorescently tagged PCR primers as follows:

5′-biotin-ctgaatcttgtagatagcta-3′   5′-FAM-tatttttgagcagtggctcc-3′
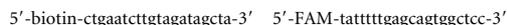
The amplification reaction (100 µl) contained 10 mM Tris-HCl (pH 8.3), 50 mM KCl, 3 mM MgCl₂, 0.2 mM each dATP, dCTP, dTTP and dGTP, 1 µM of each primer, 1 M betaine, and 5 units of AmpliTaq DNA polymerase (Perkin Elmer). In addition, 10 fmol of a 56-mer oligonucleotide identical in structure to that shown above, but containing in the variable region the non-complementary 8-mer sequence GAGACTCT, was included in the reactions. The function of this was to help equalize the amount of material that could be amplified in the various PCR reactions performed. This was found to reduce artefacts due to amplification of trace amounts of templates present in the reactions, a source of background in the 'readout' operation. PCR was performed in an PTC-200 Peltier Thermal Cycler (MJ Research, Inc.) using 25 cycles. The PCR mixture was first held at 95 °C for 1 min, followed by cycles of 95 °C for 30 s, 40 °C for 20 s and 60 °C for 1 min.

Hybridization to addressed array for 'readout'.

The DNA addressed array was prepared by methods similar to those described in ref. 31. Briefly, a gold-coated coverslip was immersed in a 0.5 mM ethanolic solution of *n*-octadecylmercaptan overnight, followed by photopatterning of the surface using an aluminium mask consisting of 1.5-mm-diameter holes with 3 mm centre-to-centre spacing. The coverslip was then immersed in 1 mM ethanolic 11-mercaptoundecanoic acid for 1 h, followed by electrostatic adsorption of a poly-L-lysine monolayer, which was maleimide-activated as described previously[21].

PCR amplification of the products of the DNA computing process yields double-stranded 56-mers with one strand biotinylated, and the other strand fluorescein-labelled. Before addressed array readout, these double-stranded PCR products were strand-separated using streptavidin-coupled magnetic beads (Dynabeads M-280, Dynal Prod. No. 112.05, 112.06 Protocol, 1997, Dynal Inc.). After strand separation, the fluorescently labelled PCR products were resuspended in hybridization buffer (HB; 2XSSPE/0.2%SDS), applied to the 16-spot addressed array and allowed to hybridize for 1.5 h at room temperature. The addressed array coverslip was washed twice in HB, 5 min per wash, followed by immersion in a beaker of HB at 37 °C for 20 min. The coverslip was then scanned using a Molecular Dynamics FluorImager 575.

Number of oligonucleotides required for scale-up.

The oligonucleotides employed for a general purpose multiple word DNA computer of the type employed here are of two types: (1) multiple word combinatorial mixtures, thiol-modified to permit surface attachment when preparing the unaddressed surface on which the computation is performed, and (2) single word individual oligonucleotides, either thiol-modified for surface attachment when preparing addressed 'readout' arrays (S$_x$s), unmodified for use in the 'mark' operation (C$_x$s), or with PCR-primer sequences appended for use in the 'readout' operation (C$_x$s with appended PCR-primer sequences). Thus a total of four sets of oligonucleotides must be synthesized. Although (as described in the text) the number of distinct oligonucleotides present in the combinatorial mixtures can be very large, a much smaller set of distinct oligonucleotide synthesis procedures is required to prepare them using split-and-pool methodology[32,33]; this is given by the product of the number of different oligonucleotide sequences per word and the number of words. In the 36-bit example provided above, this corresponds to $64 \times 6 = 384$ oligonucleotide syntheses. The number of individual oligonucleotides required for the three sets of S$_x$s and C$_x$s is given by the same product, for a total of $384 \times 4 = 1,536$; when solving a 3-SAT, in any given cycle (corresponding to a single clause) the number of C$_x$s required for the 'mark' operation is at most $(64 / 2) \times 3 = 96$.

1. Adleman, L. M. Molecular computation of solutions to combinatorial problems. *Science* **266,** 1021–1024 (1994).
2. Garey, M. R. & Johnson, D. S. *Computers and Intractability: a Guide to the Theory of NP-completeness* (Freeman, New York, 1979).
3. Adleman, L. M. Computing with DNA. *Sci. Am.* **279,** 54–61 (1998).
4. Lipton, R. J. DNA solution of hard computational problems. *Science* **268,** 542–545 (1995).
5. Guarnieri, F., Fliss, M. & Bancroft, C. Making DNA add. *Science* **273,** 220–223 (1996).
6. Ogihara, M. *Breadth First Search 3SAT Algorithms for DNA Computers* (Technical report TR 629, Department of Computer Science, University of Rochester, Rochester, New York, 1996).
7. Ouyang, Q., Kaplan, P. D., Liu, S. & Libchaber, A. DNA solution of the maximal clique problem. *Science* **278,** 446–449 (1997).
8. Seeman, N. C. *et al.* New motifs in DNA nanotechnology. *Nanotechnology.* **9,** 257–273 (1998).
9. Winfree, E., Liu, F. R., Wenzler, L. A. & Seeman, N. C. Design and self-assembly of two-dimensional DNA crystals. *Nature* **394,** 539–544 (1998).
10. Smith, L. M. *et al.* A surface-based approach to DNA computation. *J. Comput. Biol.* **5,** 255–267 (1998).
11. Frutos, A. G. *et al.* Demonstration of a word design strategy for DNA computing on surfaces. *Nucl. Acid. Res.* **25,** 4748–4757 (1997).
12. Frutos, A. G., Smith, L. M. & Corn, R. M. Enzymatic ligation reactions of DNA "words" on surfaces for DNA computing. *J. Am. Chem. Soc.* **120,** 10277–10282 (1998).

13. Cai, W. *et al.* in *Proc. 1st Annu. Int. Conf. on Computational Molecular Biology (RECOMB97)* 67–74 (Association for Computing Machinery, New York, 1997).

14. Smith, L. M. Automated synthesis and sequence analysis of biological macromolecules. *Anal. Chem.* **60**, 381A–390A (1988).

15. Fodor, S. P. A. *et al.* Light-directed, spatially addressable parallel chemical synthesis. *Science* **251**, 767–773 (1991).

16. Chee, M. *et al.* Accessing genetic information with high-density DNA arrays. *Science* **274**, 610–614 (1996).

17. Morimoto , N., Arita, M. & Suyama, A. in *Proc. DIMACS: DNA Based Computers (III)* (eds Rubin, H. & Wood, D. H.) 83–92 (American Mathematical Society, Providence, 1997).

18. Yoshida, H. & Suyama, A. in *Preliminary Proc. DIMACS: DNA Based Computers (V)* 9–20 (American Mathematical Society, Providence, 1999).

19. Schöning, U. in *Proc. 40th Annu. IEEE Conf. of Foundations of Computer Science (FOCS)* 410–414 (IEEE Computer Society, Los Alamitos, California, 1999).

20. Guo, Z., Guilfoyle, R. A., Thiel, A. J., Wang, R. & Smith, L. M. Direct fluorescence analysis of genetic polymorphisms by hybridization with oligonucleotide arrays on glass supports. *Nucl. Acid. Res.* **22**, 5456–5465 (1994).

21. Jordan, C. E., Frutos, A. G., Thiel, A. J. & Corn, R. M. Surface plasmon resonance imaging measurements of DNA hybridization adsorption and streptavidin/DNA multilayer formation at chemically modified gold surfaces. *Anal. Chem.* **69**, 4939–4947 (1997).

22. Bain, C. D. *et al.* Formation of monolayer films by the spontaneous assembly of organic thiols from solution onto gold. *J. Am. Chem. Soc.* **111**, 321–335 (1989).

23. Baskaran, N. *et al.* Uniform amplification of a mixture of deoxyribonucleic acids with varying GC content. *Genome Res.* **6**, 633–638 (1996).

24. Rees, W. A., Yager, T. D., Korte, J. & von Hippel, P. H. Betaine can eliminate the base pair composition dependence of DNA melting. *Biochemistry* **32**, 137–144 (1993).

25. Voss, K. O., Pieter Roos, K., Nonay, R. L. & Dovichi, N. J. Combating PCR bias in bisulfate-based cytosine methylation analysis. Betaine-modified cytosine deamination PCR. *Anal. Chem.* **70**, 3818–3823 (1998).

26. Farrell, R. E. DNA amplification. *Immunol. Invest.* **26**, 3–7 (1997).

27. Lyamichev, V. *et al.* Polymorphism identification and quantitative detection of genomic DNA by invasive cleavage of oligonucleotide probes. *Nature Biotechnol.* **17**, 292–296 (1999).

28. Pippenger, N. Developments in the synthesis of reliable organisms from unreliable components. *Proc. Symp. Pure Math.* **50**, 311–324 (1990).

29. Boneh, D., Dunworth, C., Lipton, R. J. & Sgall, J. DNA Based Computers II (eds Landweber, L. F. & Baum, E. B.) 163–170 (DIMACS Series in Discrete Mathematics and Theoretical Computer Science, Vol. 44, American Mathematical Society, Providence, 1999).

30. Karp, R. M., Kenyon, C. & Waarts, O. Error-resilient DNA computation. *Random Struct. Algor.* **15**, 450–466 (1999).

31. Gillmor, S. D., Thiel, A. J., Smith, L. M. & Lagally, M. G. Hydrophilic/hydrophobic patterned surfaces as templates for DNA arrays. *Langmuir* (submitted).

32. Gallop, M. A., Barrett, R. W., Dower, W. J., Fodor, S. P. A. & Gordon, E. M. Applications of combinatorial technologies to drug discovery. 1. Background and peptide combinatorial libraries. *J. Med. Chem.* **37**, 1233–1251 (1994).

33. Gordon, E. M., Barrett, R. W., Dower, W. J., Fodor, S. P. A. & Gallop, M. A. Applications of combinatorial technologies to drug discovery. 2. Combinatorial organic synthesis, library screening strategies, and future directions. *J. Med. Chem.* **37**, 1385–1401 (1994).

Figure 1 Tracer distribution. **a**, 14 months after release; **b**, 26 months after release. The red bars labelled 'INJ' mark the release site of the tracer. The contours denote the column integral of SF_6 (in nmol m^{-2}) and colours denote bottom depth. The tracer mapping procedure did not take the bathymetry into account, and hence the meridional distribution in the east in **a** appears broader than the valleys where the stations are located and which actually hold most of the tracer. The bathymetry is from Smith and Sandwell[16]. The stations are shown as white dots; those with stars are used for the sections in Fig. 2. Southerly latitude and westerly longitude are shown negative.

···

Evidence for enhanced mixing over rough topography in the abyssal ocean

J. R. Ledwell, E. T. Montgomery, K. L. Polzin, L. C. St. Laurent, R. W. Schmitt & J. M. Toole

Woods Hole Oceanographic Institution, Woods Hole, Massachusetts 02543, USA

···

The overturning circulation of the ocean plays an important role in modulating the Earth's climate. But whereas the mechanisms for the vertical transport of water into the deep ocean—deep water formation at high latitudes—and horizontal transport in ocean currents ha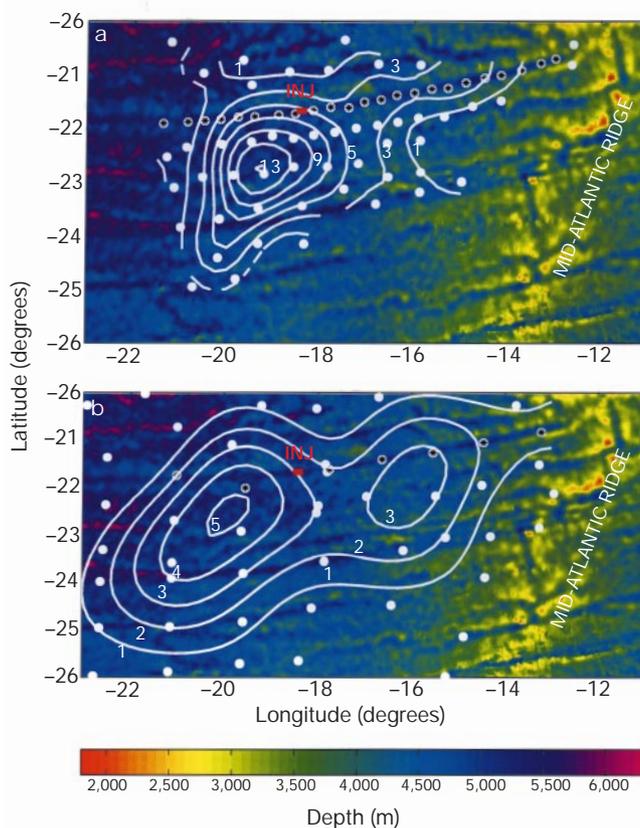ve been largely identified, it is not clear how the compensating vertical transport of water from the depths to the surface is accomplished. Turbulent mixing across surfaces of constant density is the only viable mechanism for reducing the density of the water and enabling it to rise. However, measurements of the internal wave field, the main source of energy for mixing, and of turbulent dissipation rates, have typically implied diffusivities across surfaces of equal density of only ~0.1 cm^2 s^{-1}, too small to account for the return flow. Here we report measurements of tracer dispersion and turbulent energy dissipation in the Brazil basin that reveal diffusivities of 2–4 cm^2 s^{-1} at a depth of 500 m above abyssal hills on the flank of the Mid-Atlantic Ridge, and approximately 10 cm^2 s^{-1} nearer the bottom. This amount of mixing, probably driven by breaking internal waves that are generated by tidal currents flowing over the rough bathymetry, may be large enough to close the buoyancy budget for the Brazil basin and suggests a mechanism for closing the global overturning circulation.

Our study was conducted in the abyssal Brazil basin where deep upwelling can be inferred from measurements of net inflow of dense water[4,5]. In 1996 we surveyed turbulent microstructure and internal wave fine-structure across the basin, and released 110 kg of sulphur hexafluoride above one of the zonal valleys on the western flank of the Mid-Atlantic Ridge[6] (Fig. 1). The microstructure data showed diapycnal mixing to be very low over the smooth parts of the Brazil